

# Hydrothermal Carbonization of Municipal Waste Streams: Supporting Information

*Nicole D. Berge<sup>1\*</sup>, Kyoung S. Ro<sup>2</sup>, Jingdong Mao<sup>3</sup>, Joseph R.V. Flora<sup>1</sup>, Mark A. Chappell<sup>4</sup>,*

*Sunyoung Bae<sup>5</sup>*

<sup>1</sup>Department of Civil and Environmental Engineering, University of South Carolina, 300 Main Street, Columbia, SC 29208, United States

<sup>2</sup>Coastal Plains Soil, Water, and Plant Research Center, Agricultural Research Service (ARS), United States Department of Agriculture (USDA), 2611 West Lucas Street, Florence, SC 29501, United States

<sup>3</sup>Department of Chemistry and Biochemistry, Old Dominion University, 4541 Hampton Boulevard, Norfolk, VA 23529, United States

<sup>4</sup>Environmental Laboratory, U.S. Army Corps of Engineers, 3909 Halls Ferry Rd., Vicksburg, MS 39180, USA

<sup>5</sup> Department of Chemistry, Seoul Women's University, 139-774 126 Gongreung-Dong, Nowon-Gu, Seoul, Korea

\*Corresponding author: phone: (803) 777-7521; fax: (803) 777-0670; email: [berge@cec.sc.edu](mailto:berge@cec.sc.edu)

## **Summary:**

This supporting information section presents method details; feedstock NMR spectral analysis; CSF calculations; calculations describing the volatile carbon decrease as a result of HTC; selected studies investigating hydrothermal carbonization of various feedstocks; gas composition; compounds identified in the process water and leachant solutions; results from leaching study; process water quality; relationship between HHV and hydrochar carbon content, energy to heat/evaporate water.

## ***Materials and Methods***

### **Carbonization Experiments**

Batch carbonization experiments were conducted in 160-mL stainless steel tubular reactors. Each reactor consisted of a one-inch diameter stainless steel pipe nipple and end-caps (McMaster Carr). One of the end-caps was equipped with a gas sampling valve (Swagelok, Inc.) to allow controlled collection of gas samples. Carbonization of feedstocks representing solid waste (i.e., paper, food waste, and MSW) was conducted by loading reactors with 8 g of feedstock. DI water was subsequently added to achieve a final solids concentration of 20% (wt.). AD waste was added as received. All reactors were heated at 250°C for 20 hours. After reactors were cooled, gas samples were collected and volume measured. The hydrochar was separated from the process liquid via vacuum filtration through a glass fiber filter (1  $\mu$ m, Whatman) and subsequently dried at 80°C to remove any residual moisture.

### **Analytical Techniques**

#### **Gas-Phase**

Gas samples were collected in 3-L foil gas sampling bags (SKC, Inc.). Gas volumes were measured by evacuating the gas sampling bag with a 1.0-L gas-tight syringe (Hamilton Co., Inc.). Gas samples (0.05 mL) were injected into a gas chromatograph (HP5890) equipped with a TCD and a Carboxen 1010 Plot column (30m x 0.53 mm i.d., Supelco) for determination of hydrogen concentration (carrier gas was argon). Initial oven temperature was held constant at 35°C for 7.5 min and subsequently increased to 240°C at a rate of 24°C/min. Another gas sample (0.05 mL) was injected to a GC/MS (Agilent 7890 equipped with a mass spectrometer) for determination of carbon dioxide concentration, as well as identification of other components in

the gas stream (identification via the NIST 2008 library). Gas samples for this analysis were routed through a GS-CarbonPlot column (30m long and 0.53 mm id, J&W Scientific). Initial oven temperature was 35°C. After 5-min, the temperature was increased at a rate of 25°C/min until a final temperature of 250°C was achieved. Carbon dioxide gas standards were obtained from Matheson Trigas.

### Liquid-Phase

After separating the solids from the liquid (via vacuum filtration), the liquid samples were weighed and analyzed for typical water quality parameters, including: pH, conductivity, chemical oxygen demand (COD), biochemical oxygen demand (BOD), and total organic carbon (TOC). Conductivity and pH were measured using electrodes (Thermo Scientific Orion). COD was measured using HACH reagents (HR + test kit, Loveland, CO). TOC was measured using a TOC analyzer (TOC-Vcsn, Shimadzu). BOD was measured using a respirometric technique (BODTrak II, HACH). Liquid samples were also directly (after filtration) injected to a GC/MS (Agilent 7890 equipped with a mass spectrometer) to identify compounds present in the liquid (identification using the NIST 2008 library). The liquid samples were routed through a DB-1MS column (30m x 0.25 mm id, J&W Scientific). Initial oven temperature was 40°C. After 10-min, the temperature was increased at a rate of 5°C/min until a final temperature of 300°C was achieved (following methods outlined by [1, 2]).

### Solid-Phase

After separation from the liquid, the solids were subsequently dried at 80°C to remove any residual moisture. The dried solids were weighed to determine hydrochar yields, and

subsequently sent to Hazen Research, Inc. (Golden, CO) for proximate and ultimate analyses (ASTM D3172 and 3176), along with measurement of higher heating values (HHV). To accumulate the sample mass necessary for these tests, solids were collected from at least ten replicate experiments for each individual feedstock. The reported average values represent the composite samples from ten experiments.

### <sup>13</sup>C Solid-state NMR

<sup>13</sup>C NMR analyses were performed using a Bruker Advance III 300 spectrometer at 75 MHz (300 MHz <sup>1</sup>H frequency). All experiments were run in a double-resonance probe head using 4-mm sample rotors. Two experiments, <sup>13</sup>C cross polarization/total suppression of sidebands (CP/TOSS) and <sup>13</sup>C CP/TOSS plus 40-μs dipolar dephasing, were run for each sample [3, 4]. Semi-quantitative compositional information was obtained with good sensitivity using a <sup>13</sup>C CP/MAS NMR technique (MAS = 5 kHz, CP time = 1 ms, and <sup>1</sup>H 90° pulse-length = 4 μs). Four-pulse total suppression of sidebands (TOSS) [5] was employed before detection, with a two-pulse phase-modulated (TPPM) decoupling applied for optimum resolution. Sub-spectra for nonprotonated and mobile carbon groups were obtained by <sup>13</sup>C CP/TOSS sequence with 40-μs dipolar dephasing.

### ***Leaching Experiments***

To confirm compounds detected in the process water were due to the thermal degradation process, leaching tests were performed in which each solid feedstock was placed in DI water at the concentration (20 %, wt. solids) and time (20 hrs) of the HTC experiments. Liquid samples were subsequently analyzed and compounds present identified using methods previously

described (GC-MS). Few compounds were detected (Table SI-S4), confirming the compounds detected in the process water are a direct result of thermal degradation.

### ***Explanation of Feedstock NMR Spectra***

The  $^{13}\text{C}$  CP/TOSS spectrum of rabbit food (Figure SI-S3(a)) is very similar to those of pig diets, as shown elsewhere [6]. This is understandable considering that the major components of rabbit food and pig diets (i.e., carbohydrates, lipids, and proteins) are similar. The band from 0-48 ppm arises from nonpolar alkyls such as  $\text{CCHC}$ ,  $\text{CCH}_2\text{C}$  and  $\text{CCH}_3$ , most of which are mobile as demonstrated by their significant presence in the dipolar-dephased spectrum (Figure SI-S3(b)). The shoulder around 55 ppm is primarily from  $\text{NCH}$  of proteins/peptides and mostly dephased by dipolar dephasing. The peaks around 62 ppm, 72 ppm, 85 ppm, and 102 ppm are attributed  $\text{OCH}_2$  (C6),  $\text{OCH}$  (C2, 3, 5),  $\text{OCH}$  (C4), and  $\text{O-C-O}$  (C1) of carbohydrates [7]. The almost complete removal of these signals by dipolar dephasing indicates that they are protonated (Figure SI-S3(b)). The band around 173 ppm is attributed to  $\text{COO}$  or  $\text{N-C=O}$  and cannot be dephased by dipolar dephasing. Based on these results, the major components of food are (1) carbohydrates, (2) proteins/peptides, and (3) lipids. Signals from lipids and proteins are very small compared with those of carbohydrates. The  $^{13}\text{C}$  CP/TOSS spectrum of paper shows exclusively the signals of carbohydrates (cellulose) (Figure SI-S3(e)). Again, the bands around 62 ppm, 72 ppm, 85 ppm, and 102 ppm are attributed  $\text{OCH}_2$  (C6),  $\text{OCH}$  (C2, 3, 5)  $\text{OCH}$  (C4), and  $\text{O-C-O}$  (C1) of cellulose whose signals are also removed by dipolar dephasing due to their being protonated (Figure SI-S3(f)). We do not acquire NMR spectra of mixed MSW since they are basically the stacking of the  $^{13}\text{C}$  CP/TOSS spectra of food, paper, and polyethylene terephthalate (PET) with proper proportions (45.5% paper, 16.4% plastic, and 17.6% food). The  $^{13}\text{C}$  PET spectrum has four peaks at 61.6 ppm ( $\text{OCH}_2$ ), 130 ppm (nonprotonated aromatics),

134.1 ppm (protonated aromatics), and 164.3 ppm (COO). The chemical structure of the dried AD waste is relatively complex compared with those of food and paper. It contains significantly nonpolar alkyls around 0-48 ppm, with  $\text{CCH}_3$  around 21 ppm and  $\text{C}(\text{CH}_2)_n\text{C}$  around 31 ppm (Figure SI-S3(k)). These mobile  $\text{CCH}_3$  and  $\text{C}(\text{CH}_2)_n\text{C}$  signals are retained in the dipolar-dephased spectrum (Figure SI-S3(l)). The shoulder between 40-50 ppm in the CP/TOSS spectrum is significantly reduced in the dipolar-dephased spectrum (Figure SI-S3(l)), indicative of  $\text{C}(\text{CH})\text{C}$  signals around 40 to 50 ppm. The resonances between 50-60 ppm are due to NCH of peptides or proteins, which is confirmed by disappearance of signals during this region in the dipolar dephasing spectrum. The OCH band centered around 72 ppm and especially the O-C-O peak around 105 ppm indicates the presences of carbohydrates. In addition, all the carbohydrate carbons are protonated since no signals are retained in the dipolar-dephased spectrum between 60-112 ppm. We only observe small aromatic or olefinic resonances ranging from 112 to 145 ppm. The presence of mobile olefinic  $-\text{C}=\text{C}-$  resonance around 130 ppm is evident since it also survives dipolar dephasing. Moreover, very prominent COO/N-C=O signals around 174 ppm are also observed. Based on the NMR results, AD waste contains significant (1) proteins or peptides, (2) long-chain  $-(\text{CH}_2)_n-$  of lipids, and (3) carbohydrates.

### **Carbon Storage Factor (CSF) Calculations**

As defined by Barlaz [8], the CSF is equivalent to the mass of carbon remaining within the waste following degradation/total mass of dry waste. The following expression was used to calculate the CSF associated with the HTC of each feedstock:

$$CSF = \frac{\text{Carbon remaining in char after HTC}}{\text{Mass of dry feedstock}} = \frac{\frac{\%C_{\text{Char}}}{100} * \left( \frac{\% \text{char yield}}{100} * M_{\text{feedstock}} \right)}{M_{\text{feedstock}} - \left( M_{\text{feedstock}} * \frac{\% \text{Moisture}_{\text{feedstock}}}{100} \right)}$$

Table SI-S1 contains the data used to determine the CSF associated with the HTC of each feedstock.

**Table SI-S1.** Data for calculating the CSF associated with the HTC of each feedstock.

Feedstock	% C <sub>char</sub>	M <sub>feedstock</sub> (g) <sup>1</sup>	% Char yield	% Moisture <sub>feedstock</sub> <sup>2</sup>	CSF
Paper	57.4	8	29.2	7.6	0.18
Food	67.6	8	43.8	12.6	0.34
MSW	33.5	8	63.2	6.3	0.23
AD Waste	27.8	1.2	47.1	8.1	0.14

<sup>1</sup>total wet weight of feedstock; <sup>2</sup>moisture content on a wet weight basis

### **Hydrochar Calculations**

Decreases in solid-phase volatile carbon result from the HTC of each feedstock. The reduction in volatile carbon (VC) was calculated using the following relationship:

$$\% \text{ VC Decrease} = \frac{\left[ M_{\text{feedstock}} - \left( M_{\text{feedstock}} * \frac{\% \text{Moisture}_{\text{feedstock}}}{100} \right) \right] * \frac{\% \text{VC}_{\text{feedstock}}}{100} - \left( \left( \frac{\% \text{char yield}}{100} * M_{\text{feedstock}} \right) * \frac{\% \text{VC}_{\text{char}}}{100} \right)}{\left[ M_{\text{feedstock}} - \left( M_{\text{feedstock}} * \frac{\% \text{Moisture}_{\text{feedstock}}}{100} \right) \right] * \frac{\% \text{VC}_{\text{feedstock}}}{100}} * 100$$

**Table SI-S2.** Data for calculating the %VC decrease associated with the HTC of each feedstock.

Feedstock	M <sub>feedstock</sub> (g)	% VC <sub>feedstock</sub>	% Moisture <sub>feedstock</sub>	% Char yield	% VC <sub>char</sub>	% VC Decrease
Paper	8	79.6	7.6	29.2	52.5	79
Food	8	77.6	12.6	43.8	53.4	66
MSW	8	62.0	6.3	63.2	33.6	64
AD Waste	1.2	56.0	8.1	47.1	34.5	68

**Table SI-S3.** Selected studies investigating hydrothermal carbonization of various feedstocks.

Feedstock	Temperature Range ( °C)	Reaction Time	Hydrochar Yield (%)	Catalyst Addition	% C in Char	Source
Paper drunnage	260 – 320	30 - 120 min	29 - 35	None	NR	[9]
Walnut shells	200 – 300	60 min	0 - 98	HCl, KOH, Na <sub>2</sub> CO <sub>3</sub>	23 - 102	[10]
Cellulose	330 – 380	120 min	7 - 12.4	None	30 - 40	[11]
Starch	330 – 380	120 min	4.95 - 6.21	None	20 - 25	[11]
Glucose	330 – 380	120 min	2.68 - 4.24	None		[11]
Biomass	330 – 380	120 min	4.42 - 5.79	None	16 - 21	[11]
Pine wood	280 – 340	10 - 60 min	NR	Ca(OH) <sub>2</sub> , Ba(OH) <sub>2</sub> , FeSO <sub>4</sub>	47.6 - 76.3	[12]
Wood biomass (sawdust)	280	15 min	4 - 41.7	NaOH, Na <sub>2</sub> CO <sub>3</sub> , KOH, K <sub>2</sub> CO <sub>3</sub>	NR	[1]
Wood biomass (sawdust)	180 – 280	15 - 60 min	41 - 73	Ca(OH) <sub>2</sub>	NR	[2]
Hexoses	180	24 hours	NR	None	64.15 - 65.76	[13]
Pentoses	180	24 hours	NR	None	68.6	[13]
Cellulose	230 – 250	2 - 4 hours	33.5 - 52.3	None	70.72 - 72.52	[14]
Fructose	120 – 180	0.5 - 2 hr	NR	None	NR	[15]
Pine needles, pine cones, orange peels, and oak leaves	180 – 250	16 hours	37.5 - 63.2	Citric acid	68 - 73	[16]
Tropical peat	150 – 380	30 min	53 - 98	None	57.8 - 77.8	[17]
Rabbit food	200 – 350	10 - 200 sec	30 - 50	None	NR	[18]
Wood biomass, cellulose, lignin	280	15 min	41 - 60	None	NR	[1]
Glucose	190	16 hours	NR	Acrylic Acid	NR	[19]
Glucose	160 -200	30 min	NR	Tellurium	NR	[20]
Cetyltrimethylammonium bromide	160	24 hours	NR	Ascorbic acid, AgNO <sub>3</sub>	NR	[21]
Starch	160	12 hours	NR	AgNO <sub>3</sub>	NR	[22]
Refuse derived fuel (paper, cardbaord, wood, and plastic)	300 – 375	NR	40 - 70	NaOH	36 - 56	[23]
Pinewood	300	20 min	NR	None	61.6	[24]
Microalgae	190 – 210	30 – 120 min	28 - 46	Citric or Oxalic acid	45 - 73	[25]

NR = not reported



**Table SI-S4.** Compounds identified in the HTC process water<sup>1</sup>.

Feedstock	Compounds Identified in Process Water	
	Leaching	HTC
Paper	None	1,2-Ethanediol 1,4-Benzenediol, 2-methyl- 2(3H)-Furanone, dihydro-5-methyl- 2-Cyclopenten-1-one, 2,3,4-trimethyl- 2-Cyclopenten-1-one, 2,3-dimethyl- 2-Cyclopenten-1-one, 2-methyl- 2-Cyclopenten-1-one, 3,4-dimethyl- 2-Cyclopenten-1-one, 3-methyl- 2-Hexanamine, 4-methyl- Acetic acid Butyrolactone Cyclobutanol Cyclohexane, (1-methylethylidene)- Cyclopentanecarboxaldehyde, 2-methyl-3-methylene- Cyclopentanone Cyclopentanone, 2-ethyl- Furan, 2-ethyl-5-methyl- n-Hexylmethylamine o-Methylisourea hydrogen sulfate Pentanal Piperazine Piperazine, 2-methyl- Propylene Glycol Silane, methyl- Tetrahydrofurfuryl chloride
Food	Acetic acid 2-Propanone, 1-hydroxy-	1,3,5-Triazin-2(1H)-one, 4,6-diamino- 1-Ethyl-2-methylcyclohexanol 2(3H)-Furanone, 5-ethyl-dihydro- 2,4,6-Cycloheptatrien-1-one, 2-hydroxy- 2,5-Furandicarboxaldehyde 2,5-Norbornanediol 2,5-Pyrrolidinedione, 1-butyl- 2,5-Pyrrolidinedione, 1-ethyl- 2,5-Pyrrolidinedione, 1-methyl- 2-Cyclopenten-1-one, 2,3-dimethyl- 2-Cyclopenten-1-one, 2-methyl- 2-Diisopropylaminoethyl ethyl sulfide 2-Fluoro-4-methylanisole 2H-Quinolizine, 1,3,4,6,7,9a-hexahydro- 3-Pyridinol, 6-methyl- 4-Pyridinol 5,10-Diethoxy-2,3,7,8-tetrahydro-1H,6H-dipyrrolo[1,2-a;1',2'-d]pyrazine Acetic acid Benzene, 1-fluoro-4-nitro- Cyclopentanone Hexahydroindole Hydrogen chloride Hydroquinone O-Ethyl O-2-diisopropylaminoethyl methylphosphonite Phenol Phenol, 2-methoxy-

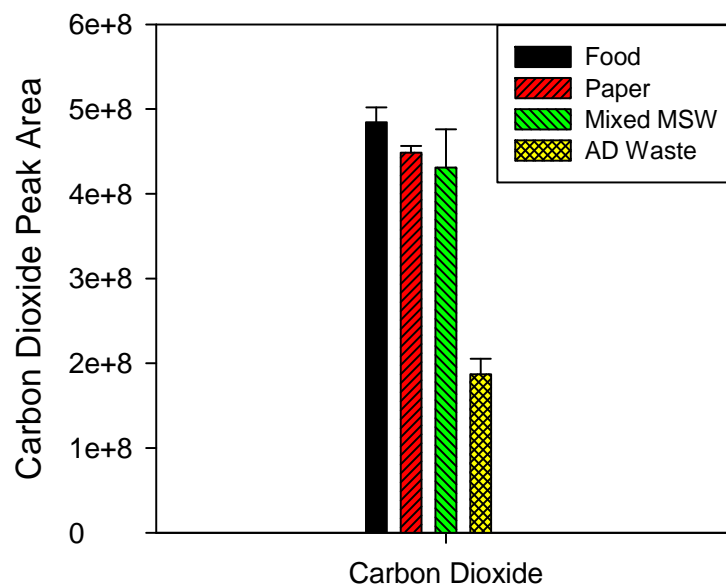
		Phenol, 2-methyl- Phenol, 3-ethoxy- Pyrazine, 2,5-dimethyl- Pyrazine, methyl- Pyrrolidine, 1-acetyl-
Mixed MSW	Acetic acid 2-Propanone, 1-hydroxy-	1,2-Benzenediol 1,2-Ethanediol 1,2-Propanediol, 3-methoxy- 1,4-Benzenediol, 2-methyl- 1-Methyl-4-[nitromethyl]-4-piperidinol 1-Methyldodecylamine 1-Phenethyl-piperidin-4-ol 1-Propanol, 2-amino- 2,5-Pyrrolidinedione, 1-ethyl- 2,5-Pyrrolidinedione, 1-methyl- 2-Acetonycyclopentanone 2-Butanamine, (S)- 2-Cyclopenten-1-one 2-Cyclopenten-1-one, 2,3-dimethyl- 2-Cyclopenten-1-one, 2-methyl- 2-Cyclopenten-1-one, 3,4-dimethyl- 2-Cyclopenten-1-one, 3-methyl- 2-Heptanamine, 5-methyl- 2-Propanamine 3-Aminopyridine 3-Buten-2-one, 3-methyl-, dimethylhydrazone 3-Cyclohexen-1-one, 2-isopropyl-5-methyl- 3-Cyclohexene-1-carboxaldehyde, 4-methyl- 4-Amino-2(1H)-pyridinone 4-Fluorohistamine 5-Ethyl-2-furaldehyde Acetic acid Benzoic acid, 2,4-dihydroxy-, (3-diethylamino-1-methyl)propyl ester Butanoic acid, 2-oxo- Butyrolactone Dimethylamine dl-Alanine Formic acid phenyl ester Hydrogen chloride Methylpent-4-enylamine Phenethylamine, p-methoxy-.alpha.-methyl-, (.+/-.)- Phenol Phenol, 4-methyl- Pyrazole, 1-methyl-4-nitro- Tetrahydro-4H-pyran-4-ol
AD Waste	None	1-Methyl-4-[nitromethyl]-4-piperidinol 1-Methyldodecylamine 1-Phenethyl-piperidin-4-ol 1-Propanol, 2-amino- 2,5-Pyrrolidinedione, 1-ethyl- 2,5-Pyrrolidinedione, 1-methyl- 2-Butanamine, (S)- 2-Cyclopenten-1-one, 2,3-dimethyl- 2-Cyclopenten-1-one, 2-methyl- 2-Heptanamine, 5-methyl-

		2-Propanamine 3-Aminopyridine 3-Buten-2-one, 3-methyl-, dimethylhydrazone 3-Cyclohexene-1-carboxaldehyde, 4-methyl- 4-Fluorohistamine Acetic acid Benzoic acid, 2,4-dihydroxy-, (3-diethylamino-1-methyl)propyl ester Dimethylamine dl-Alanine Formic acid phenyl ester Hydrogen chloride Methylpent-4-enylamine Phenethylamine, p-methoxy-.alpha.-methyl-, (.+/-.)- Phenol Phenol, 4-methyl- Pyrazole, 1-methyl-4-nitro- Tetrahydro-4H-pyran-4-ol
--	--	--

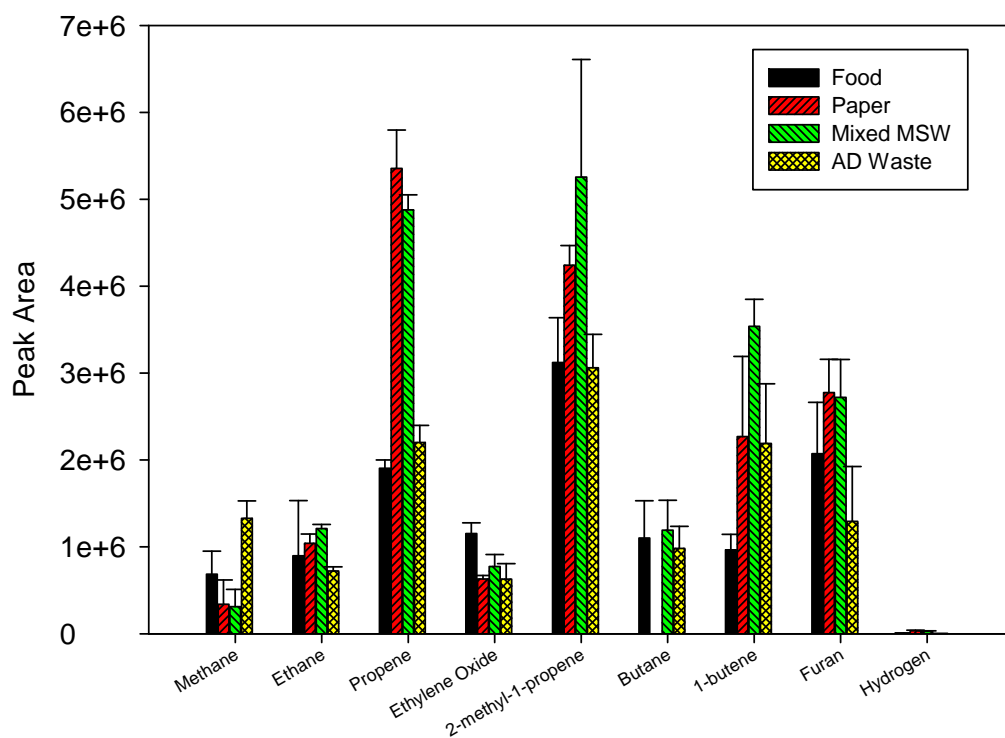
<sup>†</sup>compounds representing > 0.5% of the total peak area are included in this table; listed in alphabetical order.

**Table SI-S5.** Properties of the leachant associated with each waste material.

Feedstock	pH	COD (mg/L)	TOC (mg/L)	BOD (mg/L)
Paper	8.9	6,700	5,000	3,000
Food	6.01	38,800	35,700	27,300
Mixed MSW	7.08	8,000	6,000	4,000
AD Waste	8.91	700	100	80



(a)



(b)

**Figure SI-1.** Compounds identified in the gas following the hydrothermal carbonization of each feedstock: (a) carbon dioxide and (b) trace gases. Values represent the average of three experiments. Error bars represent the standard deviations.

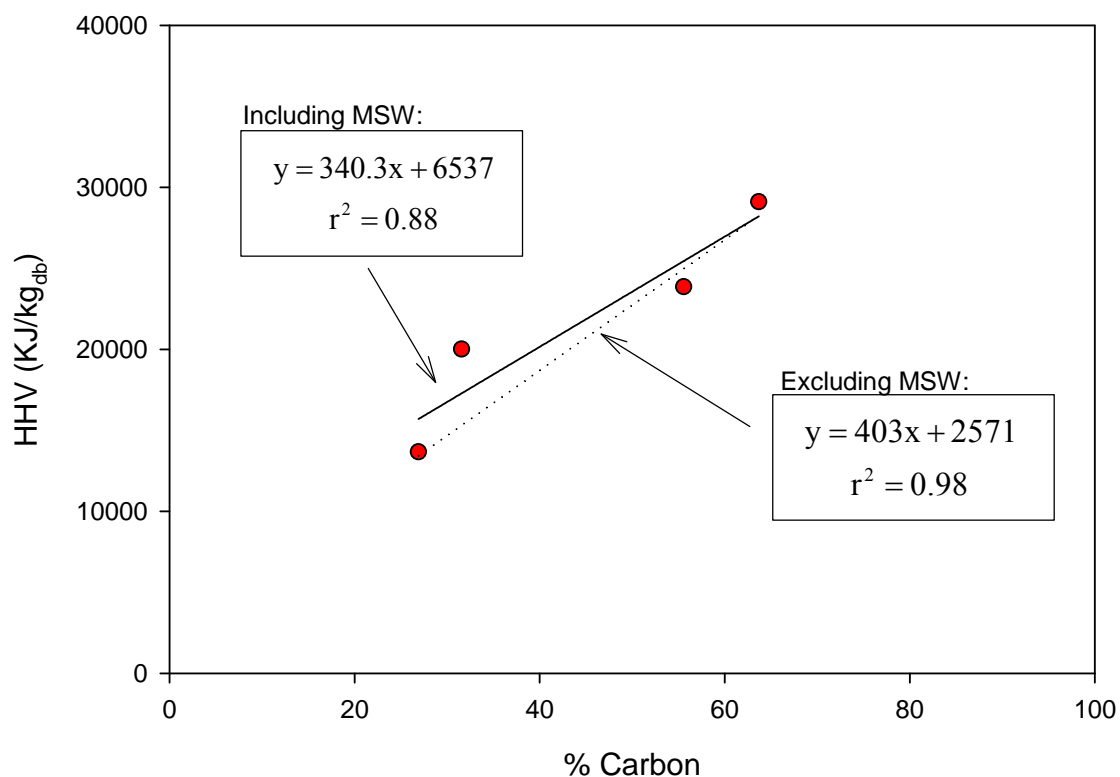


**Figure SI-S2.** Relationship between HHV and carbon content of the hydrochar solids including and excluding the MSW data.

**Table SI-S6.** Comparison of measured HHV to predicted HHV using relationship provided by Ramke et al. [26].

Waste Component	Measured HHV (KJ/kg <sub>db</sub> )	Predicted HHV (KJ/kg <sub>db</sub> ) <sup>1</sup>	% Error
Paper	23860	22594	5.3
Food	29100	25831	11.2
MSW	20010	13025	34.9
AD Waste	13660	11167	18.3

<sup>1</sup> reported by [26]:  $HHV = 398.7(\%C) + 437.88$

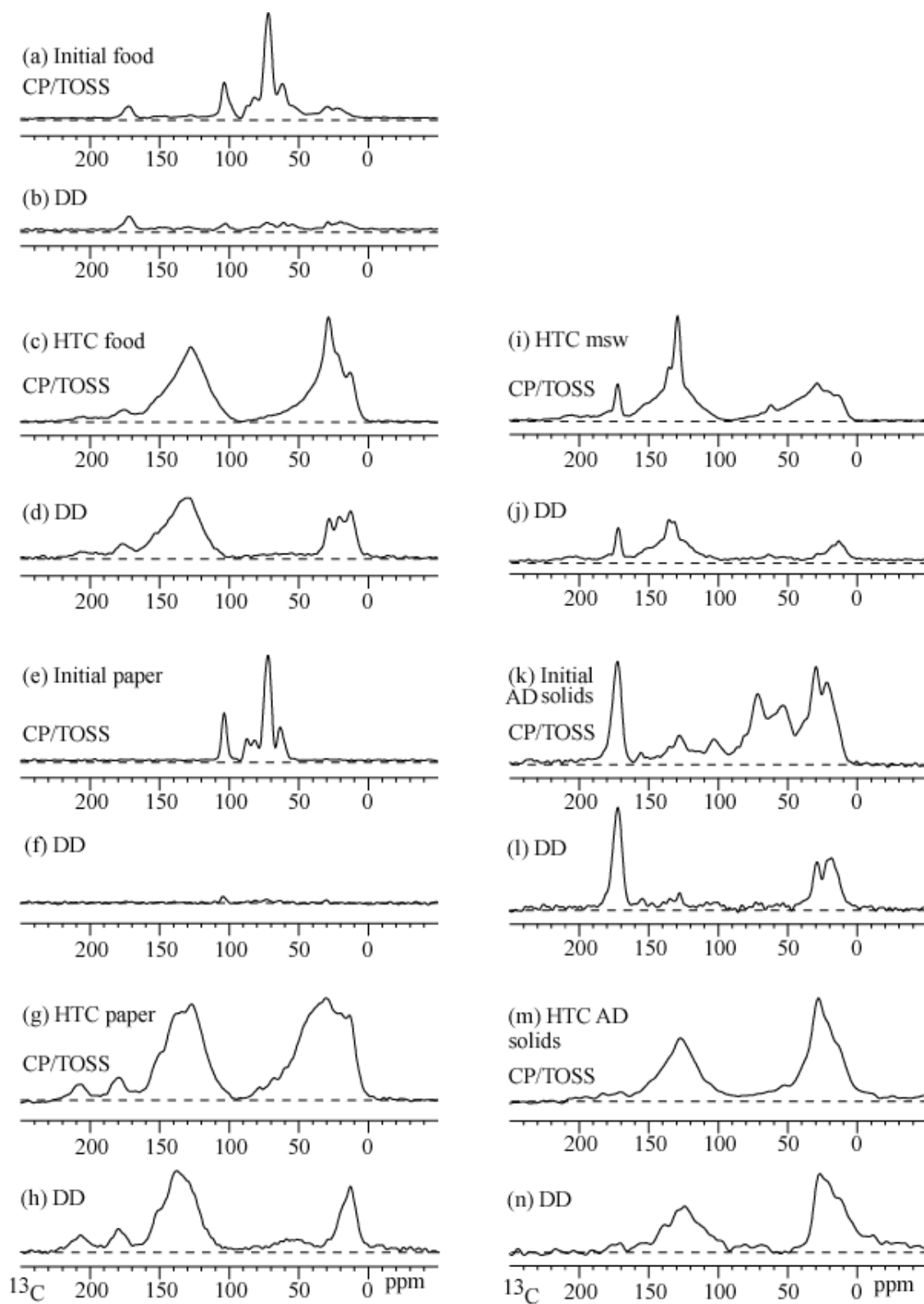


**Figure SI-S3.** The spectra of  $^{13}\text{C}$  CP/TOSS and  $^{13}\text{C}$  CP/TOSS with dipolar dephasing (DD) of food ((a) and (b)), food char ((c) and (d)), paper ((e) and (f)), paper char ((g) and (h)), MSW char ((i) and (j)), AD waste ((k) and (l)), AD waste char ((m) and (n)).

### **Calculations comparing energy required to evaporate water and energy required to heat water in a closed batch system**

The energy required to evaporate water can be calculated using:

$$E = mc_p\Delta T + mH_v$$

where m is the mass of water,  $c_p$  is the heat capacity of water,  $\Delta T$  is the change in temperature, and  $H_v$  is the heat of vaporization of water. When 32 g of water at 25 °C is heated to 100 °C and evaporated, the total energy required is 83 kJ. If the feedstock contains is comprised of 20% solids by wt. (i.e., 8g solid with 20% water), the energy required to evaporate water is 10.3 MJ/kg of feedstock.

In a closed batch system, the energy required to heat water can be calculated by accounting for the mass distribution of water at the target temperature and by evaluating the enthalpy difference of the system at the final and initial temperatures. The mass distribution of water can be calculated from:

$$m_{H_2O, total} = \rho_{H_2O, liq} V_{liq} + \rho_{H_2O, vapor} V_{gas}$$

$$V_{reactor} = V_{liq} + V_{gas}$$

where m is the mass,  $\rho$  is the density and V is the volume. The enthalpy of the system at specific temperature ( $H_T$ ) can be calculated from:

$$H_T = \rho_{H_2O, liq} V_{liq} H_{T, liq} + \rho_{H_2O, vapor} V_{gas} H_{T, vapor}$$

The energy required to heat 32 g water in a 0.16 L system from an initial temperature of 25 °C to a final temperature of 250 °C is 36 kJ. For the same feedstock comprised of 20% solids by wt., the energy required to heat the system is 4.5 MJ/kg of feedstock.

## **References:**

1. Karagoz, S.; Bhaskar, T.; Muto, A.; Sakata, Y.; Oshiki, T.; Kishimoto, T., Low-temperature catalytic hydrothermal treatment of wood biomass: analysis of liquid products. *Chem. Eng. J.* **2005**, *108*, (1-2), 127-137.
2. Karagoz, S.; Bhaskar, T.; Muto, A.; Sakata, Y.; Uddin, M., Low-temperature hydrothermal treatment of biomass: effect of reaction parameters on products and boiling point distributions. *Energy and Fuels* **2004**, *18*, 234-241.
3. Mao, J.-D.; Cory, R. M.; McKnight, D. M.; Schmidt-Rohr, K., Characterization of a nitrogen-rich fulvic acid and its precursor algae by solid-state NMR. *Organic Geochemistry* **2007**, *38*, 1277-1292.
4. Mao, J.-D.; Tremblay, L.; Gagne, J.-P.; Kohl, S.; Rice, J.; Schmidt-Rohr, K., Humic acids from particulate organic matter in the Suguenay Fjord and the St. Lawrence Estuary investigated by advanced solid-state NMR. *Geochimica et Cosmochimica Acta* **2007**, *71*, 5483-5499.
5. Dixon, W. T., NMR spectra in spinning sidebands (TOSS). *J. Chem. Phys.* **1982**, *77*, 1800-1809.
6. Mao, J.-D.; Ajakaiye, A.; Lan, Y.; Olk, D. C.; Ceballos, M.; Zhang, T.; Fan, M. Z.; Forsberg, C. W., Chemical structures of manure from conventional and phytase transgenic pigs investigated by advanced solid-state NMR spectroscopy. *Journal of Agricultural and Food Chemistry* **2008**, *56*, 2131-2138.
7. Mao, J.-D.; Holtman, K. M.; Franqui-Villanueva, D., Chemical structures of corn stover and its residue after dilute acid prehydrolysis and enzymatic hydrolysis: Insight into factors limiting enzymatic hydrolysis. *Journal of Agricultural and Food Chemistry* **2010**, *58*, 11680-11687.
8. Barlaz, M. A., Carbon storage during biodegradation of municipal solid waste components in laboratory-scale landfills. *Global Biogeochemical Cycles* **1998**, *12*, (2), 373-380.
9. Reynolds, J.; Burnham, A.; Wallman, P., Reactivity of paper residues produced by a hydrothermal pretreatment process for municipal solid wastes. *Energy and Fuels* **1997**, *11*, 98-106.
10. Lui, A.; Park, Y.; Huang, Z.; Wang, B.; Ankumah, R.; Biswas, P., Product identification and distribution from hydrothermal conversion of walnut shells. *Energy and Fuels* **2006**, *20*, 446-454.
11. Williams, P.; Onwudili, J., Subcritical and supercritical water gasification of cellulose, starch, glucose, and biomass waste. *Energy and Fuels* **2006**, *20*, 1259-1265.
12. Xu, C.; Lad, N., Production of heavy oils with high caloric values by direct liquefaction of woody biomass in sub/near-critical water. *Energy and Fuels* **2008**, *22*, 635-642.
13. Titirici, M.; Antonietti, M.; Baccile, N., Hydrothermal carbon from biomass: a comparison of the local structure from poly- to monosaccharides and pentoses/hexoses. *Green Chemistry* **2008**, *10*, 1204-1212.
14. Sevilla, M.; Fuertes, A. B., The production of carbon materials by hydrothermal carbonization of cellulose. *Carbon* **2009**, *47*, (9), 2281-2289.
15. Yao, C.; Shin, Y.; Wang, L. Q.; Windisch, C. F.; Samuels, W. D.; Arey, B. W.; Wang, C.; Risen, W. M.; Exarhos, G. J., Hydrothermal dehydration of aqueous fructose solutions in a closed system. *J. Phys. Chem. C* **2007**, *111*, (42), 15141-15145.



16. Titirici, M. M.; Thomas, A.; Yu, S. H.; Muller, J. O.; Antonietti, M., A direct synthesis of mesoporous carbons with bicontinuous pore morphology from crude plant material by hydrothermal carbonization. *Chemistry of Materials* **2007**, *19*, (17), 4205-4212.
17. Mursito, A. T.; Hirajima, T.; Sasaki, K., Upgrading and dewatering of raw tropical peat by hydrothermal treatment. *Fuel* **89**, (3), 635-641.
18. Goto, M.; Obuchi, R.; Hiroshi, T.; Sakaki, T.; Shibata, M., Hydrothermal conversion of municipal organic waste into resources. *Bioresource Technology* **2004**, *93*, (3), 279-284.
19. Demir-Caken, R.; N. Baccile; Antonietti, M.; Titirici, M., Carboxylate-rich carbonaceous materials via one-step hydrothermal carbonization of glucose in the presence of acrylic acid. *Chemistry of Materials* **2009**, *21*, (484-490).
20. Qian, H.; Yu, S.; Lou, L.; Gong, J.; Fei, L.; Lui, X., Synthesis of uniform Te@carbon-rich nanocables with photoluminescence properties and carbonaceous nanofibers by the hydrothermal carbonization of glucose. *Chemistry of Materials* **2006**, *18*, 2012-2108.
21. Fang, Z.; Tang, K.; Lei, S.; Li, T., CTAB- assisted hydrothermal synthesis of Ag/C nanostructures. *Nanotechnology* **2006**, *17*, 3008-3011.
22. Yu, S.; Cui, X.; Li, L.; Li, K.; Yu, B.; Antonietti, M.; Colfen, H., From starch to metal/carbon hybrid nanostructures: hydrothermal metal-catalyzed carbonization. *Advanced Materials* **2004**, *18*, 1636-1640.
23. Onwudili, J. A.; Williams, P. T., Hydrothermal catalytic gasification of municipal solid waste. *Energy Fuels* **2007**, *21*, (6), 3676-3683.
24. Liu, Z. G.; Zhang, F. S.; Wu, J. Z., Characterization and application of chars produced from pinewood pyrolysis and hydrothermal treatment. *Fuel* **2010**, *89*, (2), 510-514.
25. Heilmann, S. M.; Davis, H. T.; L.R., J.; Lefebvre, P. A.; Sadowsky, M. J.; Schendel, F. J.; von Keitz, M. G.; Valentas, K. J., Hydrothermal carbonization of microalgae. *Biomass and Bioenergy* **2010**, *34*, 875-882.
26. Ramke, H. G.; Blohse, D.; Lehmann, H. J.; Fettig, J. In *Hydrothermal carbonization of organic waste*, Twelfth International Waste Management and Landfill Symposium, Sardinia, Italy, 2009; Sardinia, Italy, 2009.